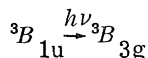


the Z axis as axis of symmetry. To measure this induced birefringence a probing beam of plane-polarized tungsten light is propagated along the laboratory Y axis, with a polarization vector inclined approximately 45° with respect to the Z axis. A $\frac{3}{4}$ -m Czerny-Turner spectrometer behind the analyzer is used to select the wavelength of interest and also serves to determine the population of the triplet state by a measurement of triplet-triplet



absorption.² For the measurement at 6328 Å a He-Ne laser was substituted for the tungsten light. The interaction of the probing light with the sample is determined by the polarizability tensor of the sample. The polarizer and analyzer are crossed when the system is completely in the ground state. Upon the orientationally selective excitation of the triplet state, the polarizability tensor is modified and the change in the polarization of the light leaving the sample is obtained. This measurement, coupled with a knowledge of the triplet-state population, allows a determination of Δ .³ For the extinction coefficient of the triplet-triplet absorption we used the value of 3.2×10^4 obtained by Brinen.⁴

After appropriate corrections were made for the environment of the deuterated naphthalene, the values for Δ at the wavelengths of 4500, 4600, and 6328 Å were found to be $\Delta_{4500} = -2.60 \times 10^{-24} \text{ cm}^3$, $\Delta_{4600} = -2.01 \times 10^{-24} \text{ cm}^3$, and $\Delta_{6328} = -0.604 \times 10^{-24} \text{ cm}^3$. Using the known

ground-state polarizabilities for naphthalene⁵ ($\alpha_x^0 = 9.6 \times 10^{-24} \text{ cm}^3$, $\alpha_y^0 = 24.4 \times 10^{-24} \text{ cm}^3$, $\alpha_z^0 = 18.2 \times 10^{-24} \text{ cm}^3$) we find for the excited state that $2\alpha_z - \alpha_y - \alpha_x$ is equal to $-0.20 \times 10^{-24} \text{ cm}^3$, $0.39 \times 10^{-24} \text{ cm}^3$, $1.8 \times 10^{-24} \text{ cm}^3$ for 4500, 4600, and 6328 Å, respectively. These values are consistent with the fact that the strongest triplet-triplet transition in the visible and ultraviolet regions is at 4148 Å and has a transition moment along the molecular y axis. Thus, α_y increases more rapidly than α_z and α_x as the wavelength decreases, and the quantity $2\alpha_z - \alpha_y - \alpha_x$ becomes smaller.

The technique used here is of course applicable to other systems and should be able to provide valuable direct information on the polarizabilities of excited electronic states. The authors wish to thank J. Duran for his assistance.

*Permanent address: Department of Physics, Simon Fraser University, Burnaby 2, British Columbia, Canada.

¹R. E. Kellogg and R. P. Schwenker, *J. Chem. Phys.* **41**, 2860 (1964); K. B. Eisenthal and M. A. El Sayed, *J. Chem. Phys.* **42**, 794 (1965).

²M. A. El Sayed and T. Pavlopoulos, *J. Chem. Phys.* **39**, 834 (1963); D. P. Craig and I. G. Ross, *J. Chem. Soc.* 1589 (1954).

³A detailed analysis of this technique showing explicitly the dependence of Δ on the measured parameters will be published.

⁴C. S. Brinen, private communication. The data were obtained using ESR to measure the triplet population.

⁵M. F. Vuks, *Opt. Spektrosk.* **20**, 644 (1966) [translation: *Opt. Spectrosc.* **20**, 361 (1966)].

STIMULATED BRILLOUIN SCATTERING: ORIGINS OF ANTI-STOKES COMPONENTS

N. Goldblatt and M. Hercher

Institute of Optics, University of Rochester, Rochester, New York 14627

(Received 5 December 1967)

Two independent mechanisms which result in the generation of anti-Stokes Brillouin components in the presence of Stokes scattering have been identified experimentally.

Strong anti-Stokes Brillouin components were recently observed by Wick, Rank, and Wiggins¹ and by Wiggins *et al.*,² at 0° to the incident laser beam in a variety of liquids. By focusing light from a 70-MW Q -switched ruby laser into a cell containing CS_2 , they recorded 42 Stokes and 20 anti-Stokes lines in the forward direction. They attribute the intense anti-Stokes

scattering to optical mixing. Both the Stokes and anti-Stokes lines were of comparable intensity with the transmitted laser line. The high intensities of the lines and their dependence on the laser power suggest very strongly that they were indeed derived from parametric amplification.

In this Letter we suggest a number of other mechanisms for the generation of intense anti-Stokes Brillouin components, and cite experimental evidence which confirms the existence of one of these. We found that under the usu-

al experimental conditions, the four-photon parametric process (optical mixing) proposed by Wiggins was the dominant source of anti-Stokes Brillouin components, but that under certain conditions a photon-phonon process dominated. The forward-traveling Stokes components arise from the amplification and reflection of the backscattered Stokes radiation by the laser. When the n th Stokes component returns to the sample, it produces the $(n + 1)$ th backscattered Stokes component. The process can occur many times since a large percentage of incident radiation is converted into Stokes radiation at each step. The high scattering efficiency is the result of parametric amplification of both the Stokes-photon and thermal-phonon fields. This in turn comes about because each Stokes scattering involves the addition of a phonon to the scattering field already present.

The experimental data on intense anti-Stokes scattering are more difficult to interpret unambiguously. Since the creation of an anti-Stokes photon requires the annihilation of a phonon, it is clear that such a scattering event provides no gain for the associated phonon field as was the case for Stokes scattering. On the other hand, intense photon field at the laser frequency plus the intense phonon field associated with stimulated Stokes scattering provide a poten-

tial source of intense anti-Stokes scattering even in the absence of a direct gain mechanism.

The investigations of Wick, Rank, and Wiggins and Wiggins *et al.*, leave open to question the possible role of photon-phonon interactions of this type in the generation of anti-Stokes Brillouin radiation. It was the purpose of the present investigation to answer this question.

Figure 1 lists various possible sequences for producing the phonon and photon fields in the directions appropriate to produce anti-Stokes light in the forward spectrum. The frequency of each component appears above its momentum vector. In sequence I, incident laser radiation (ω_0) produces 180° stimulated Stokes radiation (ω_{-1}). The next interaction involves the production of a 180° phonon field to produce 180° anti-Stokes radiation (ω_{+1}). Finally, the laser reflectors or a mirror placed between the laser and the sample serve to reflect ω_{+1} into the forward direction. The other sequences are interpreted similarly.

There are basically two types of interactions, shown in Fig. 1. Sequences I through IV involve the interaction of a laser photon and a phonon traveling in opposite directions. They combine to generate an anti-Stokes photon traveling in the direction of the phonon [interaction (Ic), (IIb), (IIIb), or (IVb)]. The other type of interaction is a parametric four-photon scattering process

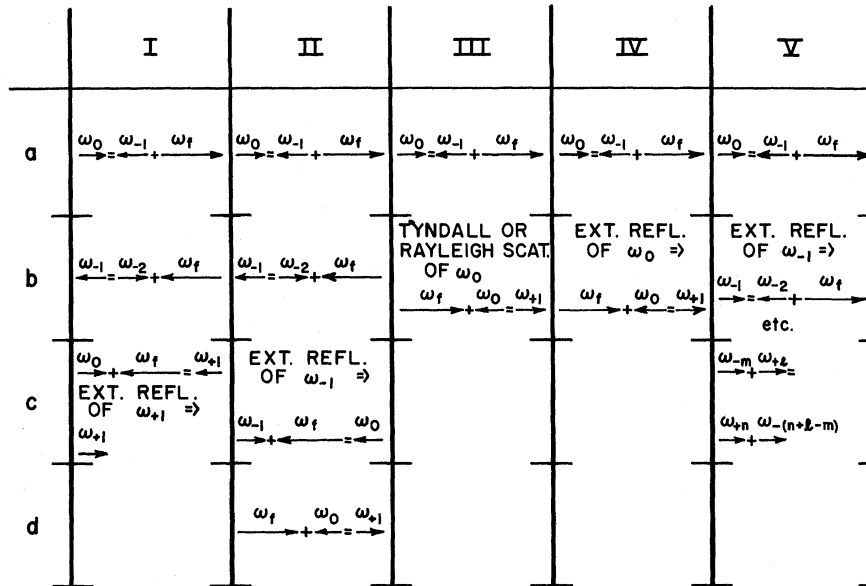


FIG. 1. Possible mechanisms for production on intense anti-Stokes Brillouin components. $\omega_0 = \omega_0 + n\omega_f$ is the frequency of the n th Stokes ($n < 0$) or anti-Stokes ($n > 0$) line. ω_0 and ω_f are laser and phonon frequencies, respectively. Since $k_f \approx 2k_n$ for 180° scattering, arrows which represent momenta are to scale. Sequences are denoted by Roman numerals and interactions proceed downward—*a*, *b*, *c*, etc.

such as (Vc). In this instance, the laser light and various Stokes components (which have been reflected into the forward direction by the laser mirrors) combine in the scattering medium and anti-Stokes radiation is generated. For example, two laser photons can combine to produce anti-Stokes and Stokes photons. [In interaction (Vc), $m = l = 0, n = 1$.] Similarly, a laser photon can combine with a first-order Stokes photon to produce a second-order Stokes and an anti-Stokes photon ($m = 1, l = 0, n = 1$), and so on. This is exactly analogous to the production of anti-Stokes components in the stimulated Raman effect. In the Brillouin case, however, since the frequencies of the various components are so closely spaced ($\sim 0.2 \text{ cm}^{-1}$), momentum matching occurs in the forward direction instead of in cones around the forward direction as in the Raman experiment. It is stressed that photon-phonon interactions involving generation of anti-Stokes radiation do not involve gain. However, they are assumed to result in a detectable (interferometrically) anti-Stokes signal, since in each case the participating phonon field is strong, being produced by a stimulated Stokes scattering.

The experimental arrangement used to differentiate between mechanisms I-V is illustrated in Fig. 2. Using a 25-cm lens (L), with an 8-mm aperture, linearly polarized light from a single-frequency ruby laser, operating with an output of 25 MW/cm^2 was focused near the center of a 50-cm scattering cell. Toluene, carbon disulfide, and hexane were used as scattering media. Forward and backscattered light and light returned to the interaction region was examined spectroscopically using beamsplitters B , mirror M , and Fabry-Perot interferometers. Since the Stokes and laser components were quite strong, care was taken to define the observation angles closely so as to

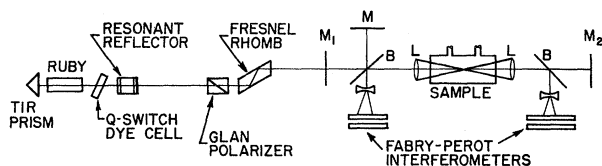


FIG. 2. Experimental configuration. Beamsplitters B and mirror M sampled 20% of incident, backscattered, and forward-scattered radiation for spectral analysis. Focusing lenses L were typically 25-cm focal length. Mirrors M_1 and M_2 and Fresnel rhomb were employed in various combinations. So as not to change the incident flux, mirrors were misaligned rather than removed when feedback was not desired.

collect scattering from cell wall and windows. Mirrors M_1 ($R_1 = 55\%$) and M_2 ($R_2 = 40-99\%$) provided feedback for backward- and forward-scattered radiation, respectively. These mirrors were aligned or misaligned depending on whether feedback in a particular direction was desired. An optical isolator consisting of a $\frac{1}{4}$ -wave retarder and polarizer served to control feedback of 180° radiation by the laser. Several experimental variations were investigated employing different combinations of feedback and isolation.

In the first experiment, the isolator was not employed, and M_1 and M_2 were misaligned. This corresponds to experimental configuration of Wick, Rank, and Wiggins and Wiggins *et al.* We observed as many as two anti-Stokes and seven Stokes order in the forward direction. It was determined that the anti-Stokes radiation originated in the sample, traveled in the forward direction, and was not initially backscattered and then reflected by the laser mirrors. Thus, the appearance of anti-Stokes radiation in this case did not involve sequence I since interaction (Ic) generates a 180° anti-Stokes photon field which was not observed.

If sequence III were playing a role, the anti-Stokes radiation should be observable without any external feedback. Therefore, the next experiment employed the optical isolator to eliminate laser feedback and both M_1 and M_2 were misaligned. In this case there was no observable anti-Stokes radiation in either the forward or backward direction. Thus sequence III was not contributing. Interaction (IIb) or (Ib) should also occur independent of external feedback. The signature of this interaction, namely second-order Stokes radiation in the forward direction in the absence of external feedback, was not observed, and only a first-order Stokes line appeared traveling backwards.³ Thus the 180° phonon field required for interaction (Ic) or (IIc) was not being generated, and sequence I and II could not be contributing anti-Stokes radiation. Sequence IV certainly was not contributing in the first experiment, since interaction (IVb) requires external feedback of transmitted laser light. This must be supplied by M_2 which was misaligned. This leads us to our conclusion that the appearance of anti-Stokes radiation in the forward direction in the presence of laser feedback is due to sequence V which does not involve phonons explicitly. External feedback serves to reflect

180° Stokes components into the forward direction, as is required in process (Vc).

To make certain that the anti-Stokes radiation was not the result of some anomalous effect due to cavity resonances, gain of laser, or polarization of incident light, the optical isolator was placed in front of the laser. Mirror M_1 was then aligned so as to return 180° scattered radiation to the interaction region. Anti-Stokes radiation was again observed in the forward direction, despite the fact that the laser was isolated from backscattered radiation. Thus we conclude that when the laser participates in the production of anti-Stokes radiation, it serves only to reflect backscattered radiation into the forward direction, as assumed.

Although we failed to observe anti-Stokes generation by sequences I, II, or III, it was possible to generate an easily detectable anti-Stokes line via sequence IV. A laser photon is externally reflected by mirror M_2 into the backward direction. It then interacts with the strong phonon field produced by primary Stokes scattering. This results in an intense anti-Stokes component in the forward direction, even without gain. To observe this effect, mirror M_2 was aligned to return the transmitted laser light to the interaction region. The laser was isolated from backscattered radiation, and mirror M_1 was misaligned in order to eliminate anti-Stokes radiation from sequence V. An easily detectable anti-Stokes line was visible in the forward direction. The transmitted laser line and a Stokes line which resulted from stimulated Stokes scattering of the reflected laser light were also observed in the forward direction. Since this intense forward-traveling Stokes light is the result of parametric amplification of scattering from a weak thermal-phonon field, it depends exponentially on the reflected laser intensity.⁴ In contrast, the intensity of the anti-Stokes light observed in this case is the result of scattering from the existing strong phonon field generated by primary Stokes scattering and thus depends linearly on reflected laser intensity.⁵ By varying the reflectivity of M_2 , we were able to observe these dependences qualitatively and thus further substantiate our conclusion in this case. A variation in R_2 of approximately 40% caused large variations in the relative intensities of forward-traveling Stokes and anti-Stokes lines. A value for R_2 could be found for a given inci-

dent intensity below which the Stokes line was too weak to be detected while the anti-Stokes line was still clearly visible. The interferograms in Fig. 3 illustrate this effect. They display the forward spectrum in toluene. In Fig. 3(a) both anti-Stokes and Stokes lines are visible, while in Fig. 3(b) feedback was insufficient to produce detectable stimulated Stokes radiation from the reflected laser light yet the anti-Stokes line is still visible. Incident laser intensity was only 1 MW over an aperture of 4 mm, focused in the sample with a 25-cm focal length lens.

We conclude that when intense laser light is focused in a liquid, forward-traveling anti-Stokes components are the result of a four-photon parametric interaction in agreement with the conclusion of Refs. 1 and 2. We have shown that the participating fields are the laser and various orders of stimulated Stokes radiation, reflected into the forward direction by the laser. Phonon annihilation does not contribute detectable anti-Stokes radiation in the above instance, although we have generated a strong anti-Stokes component by reflecting the transmitted portion of the laser light backwards into the interaction area.

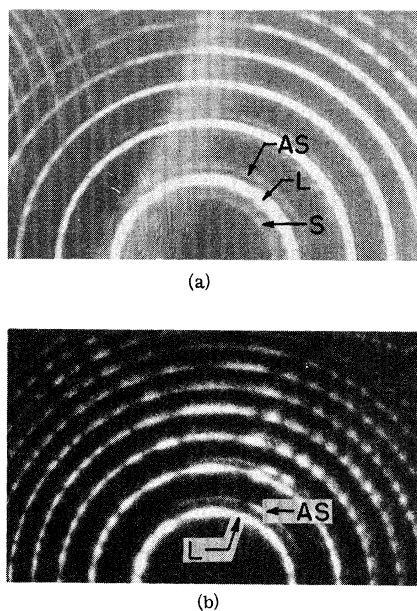


FIG. 3. Interferograms of forward-scattered light showing anti-Stokes component generated by sequence (IV). (a) Enough laser light was reflected back into the sample via M_2 to exceed threshold for Stokes scattering. (b) Reflected laser light was insufficient to produce detectable stimulated Stokes emission. Exposures were different in (a) and (b).

*This research was sponsored by the U. S. Army Research Office under Contract No. DA 31 124 ARO D 401.

¹R. V. Wick, D. H. Rank, and T. A. Wiggins, Phys. Rev. Letters **17**, 466 (1966).

²T. A. Wiggins, R. V. Wick, N. D. Foltz, C. W. Cho, and D. H. Rank, J. Opt. Soc. Am. **57**, 661 (1967).

³This result may be in contradiction to the work by Wiggins *et al.* (Ref. 2) and I. L. Fabelinskii and V. S. Starunov, Appl. Opt. **6**, 1793 (1967). They observed forward-traveling Stokes components even when the laser was isolated from the sample. They employed either an optical isolator or a long laser to sample dis-

tance or both. We observed this also. However, it was determined that, in our case, these components were due to stray reflections and incomplete absorption of the Stokes light by the quarter-wave retarder. Stray reflections were eliminated by narrowing the acceptance angle of the interferometers. Mirror M_1 provided enough double pass attenuation to render the small amount of Stokes light passed by the isolator, unobservable in the forward direction.

⁴C. L. Tang, J. Appl. Phys. **37**, 2945 (1966).

⁵M. G. Cohen and E. I. Gordon, Bell System Tech. J. **44** (1965).

PULSE-STIMULATED EMISSION FROM PLASMA COLUMNS*

D. E. Baldwin, D. M. Henderson, and J. L. Hirshfield

Department of Engineering and Applied Science, Yale University, New Haven, Connecticut

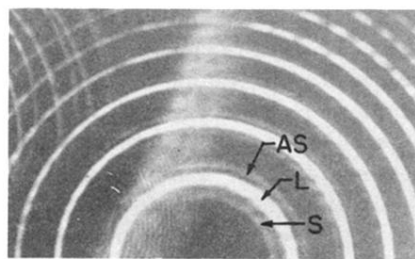
(Received 29 December 1967)

Experiment and theory are presented to show that pulse excitation of a cylindrical plasma produces decaying ringing at the electron-cyclotron frequency and at any upper hybrid frequency for which the electron-concentration gradient vanishes. In the absence of a dc magnetic field, the ringing occurs at the maximum plasma frequency.

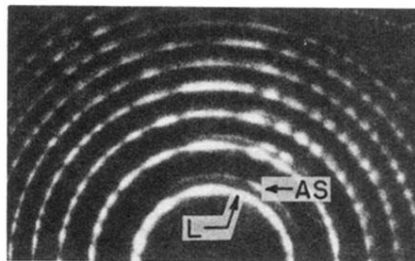
Interest has arisen lately in the transient emission from a plasma stimulated by externally applied pulses.¹⁻⁴ In particular, experiments have been described³ in which emission following excitation by a microwave pulse gave rise to a decaying ringing signal at what was identified as the upper hybrid resonance frequency ω_{uh} . The work reported in this Letter has some features in common with that of Ref. 3, but offers more extensive experimental evidence to support the following theoretical prediction (derived below): For cylindrical plasmas with equilibrium gradients only in the radial direction, the time-asymptotic oscillations following pulse excitation will occur at discrete frequencies which equal the electron-cyclotron frequency ω_c and any upper hybrid frequency $\omega_{uh}(r) = [\omega_c^2 + \omega_p^2(r)]^{1/2}$ for which $d\omega_{uh}/dr = 0$. In addition to the presentation of data on plasmas in a dc magnetic field, we also present results on a magnetic-field-free plasma to support an extension of the theory to this case. These latter data are, to our knowledge, the first reported on pulse-stimulated oscillations of magnetic-field-free plasma. The results we report suggest a simple and relatively precise method for measuring, by external means, the maximum electron concentration in plasmas in either the presence or absence of dc magnetic fields.

The experiments have been conducted in the afterglows of pulsed discharges produced by

capacitively coupling 90-MHz rf power externally to gas-filled 11-mm i.d. quartz tubes. Argon, neon, and helium have been used with pressures in the range of a few mTorr. For the experiments using the dc magnetic field \vec{B} , the discharge tube is placed in a section of RG 48/U S-band waveguide, oriented axially in a solenoid magnet and so that \vec{E}_{rf} is perpendicular to \vec{B} . The B field is homogeneous to ± 1 part in 10^4 over the plasma volume. Microwave pulses at 3.2 GHz are created by grid-modulating a traveling-wave-tube amplifier, and typical pulses have $E_{rf} = 10$ V/cm with a half-power width of 5 nsec. Plasma emission is received by a wide-band microwave amplifier with a 4-dB noise figure. The emission can be analyzed in time by homodyne detection, phase-locked to the phase of the input pulses, or can be analyzed in frequency using a spectrum analyzer. Figure 1(a) shows the frequency spectrum following a pulse at a fixed time in the afterglow. (The decay of the stimulated emission takes place on a time scale of about 50 nsec, so that the afterglow can be considered stationary on the time scale of a given pulse and the subsequent emission.) Both emission lines have been observed to be displaced linearly in frequency with variation in the dc magnetic field, and the line separation measured is proportional to electron density, as determined by independent cavity measurements. This latter dependence is expected when ω_p^2



(a)



(b)

FIG. 3. Interferograms of forward-scattered light showing anti-Stokes component generated by sequence (IV). (a) Enough laser light was reflected back into the sample via M_2 to exceed threshold for Stokes scattering. (b) Reflected laser light was insufficient to produce detectable stimulated Stokes emission. Exposures were different in (a) and (b).